Moisture Fluctuations Modulate Abiotic and Biotic Limitations of H₂ Soil Uptake

Matteo B. Bertagni[1] [ID]**, Fabien Paulot[2]** [ID]**, and Amilcare Porporato[1,3]**

[1]The High Meadows Environmental Institute, Princeton University, Princeton, NJ, USA, [2]Geophysical Fluid Dynamics Laboratory, National Oceanic and Atmospheric Administration, Princeton, NJ, USA, [3]Department of Civil and Environmental Engineering, Princeton University, Princeton, NJ, USA

Abstract Soil uptake by H_2-oxidizing bacteria is the main sink of the global hydrogen cycle, accounting for nearly 80% of the atmospheric H_2 consumption. Although the H_2 uptake is strongly influenced by soil moisture, little attention has been paid to coherently couple the water and hydrogen dynamics in soils. Toward this goal, we improve the mechanistic representation of the H_2 uptake as a function of soil moisture and highlight the role of the moisture temporal fluctuations on the biotic consumption of H_2. The results show that, due to the strongly nonlinear relationship between soil moisture and H_2 uptake, addressing the dry-wet sequences is necessary to characterize the H_2 uptake in semi-arid regions correctly. From novel analytical relationships validated with field data, we also infer the biotic and abiotic limitations in the global soil H_2 uptake. It is shown that, diffusion generally limits the uptake in humid temperate and tropical regions, while biotic limitations tend to occur in very arid or cold soils. Finally, we discuss the implications that climate change may have on the H_2 soil sink.

Plain Language Summary While hydrogen (H_2) is gaining international attention as an energy carrier with low carbon footprint, a more H_2-centered economy may also increase the H_2 atmospheric concentration, causing indirect global warming effects (e.g., increasing methane lifetime). The greatest uncertainty of H_2 future projections is related to the soil uptake by bacteria, which is widespread worldwide and accounts for nearly 80% of the H_2 atmospheric removal. As soil moisture is a major driver of the H_2 uptake, we here show the crucial influence of the temporal variability of soil moisture on the H_2 soil uptake. We demonstrate that, addressing the dry-wet sequences is necessary to correctly characterize the H_2 soil uptake in semi-arid regions, where the intermittent water availability transiently activates the bacterial activity. We also show that, H_2 diffusion through the soil generally limits the H_2 uptake in humid regions, while biotic limitations tend to occur in hyperarid soils where bacteria suffer the lack of water. Understanding how these limitations will evolve due to climate change remains an open question.

1. Introduction

Hydrogen (H_2) is the second most abundant reactive trace gas in the troposphere, after methane, with an average concentration of $\simeq$530 ppb (Novelli et al., 1999). With a progressive shift toward a more hydrogen-centered economy (Hydrogen Council, 2020; IEA, 2019), unavoidable leaks to the atmosphere are expected to increase the H_2 concentration. Although H_2 is not directly a greenhouse gas, its atmospheric oxidation—through ·OH—might produce indirect global warming effects, for example, increased lifetime of methane and stratospheric cooling (Paulot et al., 2021; Tromp et al., 2003; Warwick et al., 2004). As a result, the tropospheric budget of H_2 has gained renewed interest during the last decade (see among others Yashiro et al. (2011), Morfopoulos et al. (2012), Pieterse et al. (2013), Derwent et al. (2020), Paulot et al. (2021) and the comprehensive review by Ehhalt and Rohrer (2009)).

A peculiar feature of the H_2 tropospheric cycle is that soil uptake by bacteria accounts for nearly 80% of the tropospheric removal (Ehhalt & Rohrer, 2009; Khalil & Rasmussen, 1990; Novelli et al., 1999; Rhee et al., 2006). Practically all soils from a broad range of ecosystems worldwide have been found to uptake hydrogen (Conrad & Seiler, 1980, 1985; Lallo et al., 2008; Meredith et al., 2017; Schmitt et al., 2009; Simmonds et al., 2011; Smith-Downey et al., 2008; Yonemura, Kawashima, & Tsuruta, 2000), even in extreme environments (Ji et al., 2017; Jordaan et al., 2020).

From a biotic perspective, the uptake is mediated by H_2-oxidizing bacteria that use various kinds of hydrogenase enzymes to catalyze the break up of the H_2 molecule (Greening et al., 2015; Lubitz et al., 2014). The microbial
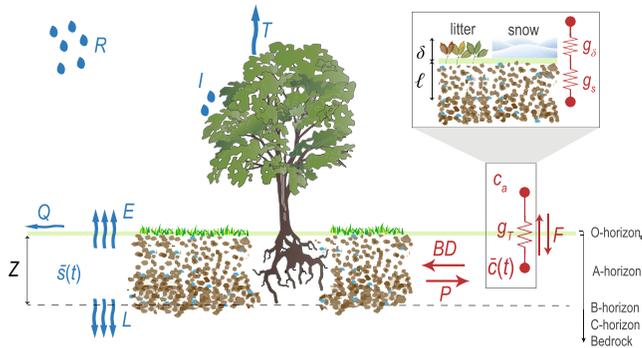
Figure 1. Sketch of the water (light blue) and hydrogen (red) depth-averaged balances in the top layers of soil. The inset shows the contribution of the diffusive barrier (g_δ) and the topmost soil layer (g_s) to the total conductance (g_T).

characterization of the H_2-oxidizing bacteria has advanced considerably in recent years (see Constant et al. (2009, 2010); Piché-Choquette and Constant (2019) and the review by Greening et al. (2015)). More interestingly, increasing evidence (Ji et al., 2017; Leung et al., 2020; Meredith et al., 2014) suggests that low consumption of atmospheric H_2 provides dormant bacteria sufficient energy to cope with adverse environmental conditions (e.g., a drought).

Among the various abiotic (e.g., temperature and soil texture) and biotic (e.g., composition of the microbial communities) factors, there is general agreement that soil moisture plays the main role in controlling the H_2 soil uptake (Conrad & Seiler, 1981; Ehhalt & Rohrer, 2011; Schmitt et al., 2009; Smith-Downey et al., 2006). The reason is that soil moisture strongly affects both the bacterial metabolism, that is, the rate at which H_2 is consumed, and the H_2 diffusion through the soil air, that is, the rate at which H_2 becomes available for bacterial consumption. Note that due to the low solubility of H_2 in water (Sander, 2015), hydrogen is found in soils mainly as a gas within the air phase. It has been shown (Conrad & Seiler, 1981; Ehhalt & Rohrer, 2011; Smith-Downey et al., 2006) that at very low and high level of soil moisture, the soil H_2 uptake is very limited; in between, there is an optimal moisture value that maximizes the H_2 soil uptake. Hence, physical and biotic processes concur to create a strongly nonlinear relationship between H_2 uptake and soil moisture.

Because soil moisture exhibits temporal fluctuations driven by the hydroclimatic forcings, its nonlinear control on the H_2 uptake may induce large temporal variations in the capacity of soil microorganisms to consume H_2. Neglecting these fluctuations could lead to large errors in the estimates of the H_2 soil uptake and consequently in the long-term predictions of global climate models.

The main goal of the present paper is to provide a modeling framework that blends process-based representations of ecohydrological and biogeochemical dynamics, capable of capturing the key nonlinearities of the soil moisture forcing on the H_2 soil uptake. We start from the spatially explicit mass balances of water and hydrogen in soils to derive a coupled system of depth-averaged equations (Section 2.1). The equation for the soil moisture dynamics explicitly resolves the soil moisture fluctuations induced by intermittent rain events and is used when soil moisture measurements are not readily available. The hydrogen dynamics accounts for the diffusive flux between the atmosphere and the soil (Section 2.2) and the biological H_2 consumption and production in the topmost layers of soil (Section 2.3). Results (Section 3) are presented in terms of temporal dynamics and probability density functions for soil moisture and H_2-related quantities (e.g., the deposition velocity v_d). We highlight the impact of soil moisture fluctuations to the H_2 uptake (Sections 3.3–3.4) and discuss the implications for global climate models (Section 4.1). From a novel analytical relationship for the deposition velocity v_d (Section 3.2), we also provide fresh insights on the abiotic and biotic limitations to the H_2 soil uptake and their relation to the different hydroclimatic regions (Section 4.2). Perspectives on future research are discussed (Section 5).

2. Model

This section provides the modeling aspects of the coupled water and hydrogen dynamics in soil. Figure 1 shows a sketch of the physical processes involved. The governing equations are introduced in Section 2.1. Diffusive flux and biological consumption of H_2 as a function of soil moisture are modeled in Sections 2.2 and 2.3, respectively.

2.1. Coupled Soil Hydrogen and Water Dynamics

Assuming horizontal homogeneity, the balance equation for H_2 in soil air may be written as,

$$\partial_t(\Theta c) = -\partial_z \phi + p - bd, \tag{1}$$

where t is time and z is the vertical direction (pointing downward), $c(z, t)$ (moles/cm$^3_{air}$) is the concentration of hydrogen in the soil air and $\Theta(z, t)$ is the soil volumetric air content (cm$^3_{air}$/cm$^3_{soil}$). The product $c\Theta = c_s$ (z, t) (moles/cm$^3_{soil}$) gives the concentration of hydrogen in a soil volume. The term $\phi = \phi(c, \theta, \delta)$ is the flux of H_2

between the atmosphere and the soil, which, as later shown, mainly depends on the concentration c, the water volumetric content $\theta(z, t)$, and the depth δ of a possible diffusive barrier (e.g., litter or snow); p is the soil production term, for example, through anaerobic fermentation or nitrogen fixation (Conrad & Seiler, 1980); bd is the biological consumption by H_2-fixing bacteria, which is a poorly constrained function of H_2 concentration, temperature, pH, soil salinity, bacteria abundance, soil carbon, and water content (Conrad & Seiler, 1981; Smith-Downey et al., 2006; Khdhiri et al., 2015). Equation 1 is coupled to the soil water balance equation (e.g., Yin et al., 2019),

$$\partial_t \theta = -\partial_z \psi - \sigma(z), \tag{2}$$

where ψ is the vertical water flux per unit area, and $\sigma(z, \theta)$ is the plant uptake.

Both Equations 1 and 2 are valid at the so-called Darcy (macroscopic) length-scale. Depending on soil texture, the Darcy scale can range from few centimeters to decimeters and it defines the smallest scale at which the continuum hypothesis holds. In the presence of well-defined soil horizons, wherein the chemical, biological and physical properties can be considered relatively homogeneous, these equations can be vertically averaged for convenience of description. Soils that have been made vertically homogeneous by agricultural practices, or where the presence of macroporosity and roots favor the soil water redistribution action, are also suitable for the depth-averaged approach. The topmost O-horizon (i.e., the litter layer) is typically rather dry and with negligible biological consumption (Yonemura, Yokozawa, et al., 2000). As a result, it acts as a barrier to H_2-fluxes to and from the atmosphere (Ehhalt & Rohrer, 2013; Yonemura, Yokozawa, et al., 2000). Most of the biological activity occurs within the A-horizon.

By integrating the previous system (1)–(2) over a depth Z (see Section S1 in Supporting Information S1 for details), and using $\theta = n s$ and $\Theta = n (1 - s)$, respectively, where $s (z, t)$ is the relative soil moisture ($s = 0$ for dry soil and $s = 1$ for saturated soil) and n is the porosity ($\theta + \Theta = n$), one obtains,

$$n Z \partial_t \bar{s} = R + J - I - Q - ET - L, \tag{3}$$

$$n Z \partial_t [(1 - \bar{s})\bar{c}] = F + Z(P - BD), \tag{4}$$

where $\bar{\cdot}$ denotes the average over the depth Z (Figure 1). In Equation 3, $R(t)$ is rainfall, $J(t)$ is irrigation, $I(t)$ is the canopy interception, $Q(s)$ is the surface runoff, $ET(s)$ is the evapotranspiration loss along the depth Z, and $L(s)$ is leakage. In Equation 4 for the depth-averaged H_2 concentration (note that $n(1 - \bar{s})\bar{c} = \bar{c}_s$), F is the flux of H_2 between the soil and the atmosphere (positive if going into the soil), P and BD are the depth-averaged H_2 production and biological decay within the soil layer. Note that to emphasize the role of the temporal fluctuations of soil moisture on the hydrogen dynamics, we will later use the moisture Equation 3 or directly field measurements of soil moisture when available.

2.2. H_2 Diffusive Flux

The H_2 flux from the atmosphere boundary layer, through the canopy, the litter (or snow) layer and eventually the soil is modeled using an electric analogy with conductances (Figure 1),

$$F = \varrho \, g_T (c_a - \bar{c}), \tag{5}$$

where c_a is the atmospheric concentration of H_2, and g_T is the total conductance. The latter is the series of the canopy-atmospheric conductance, the conductance of possible diffusive barriers (such as the litter layer or the snow cover), and the soil conductance. Since the canopy-atmospheric conductance is generally much higher than the soil conductance (see Section S2 and Figure S1 in Supporting Information S1), the total conductance can be evaluated as,

$$\frac{1}{g_T} = \frac{1}{g_\delta} + \frac{1}{g_s}, \tag{6}$$

where g_δ is the conductance of the diffusive barrier and g_s is conductance of the soil (see inset in Figure 1).

Neglecting advective fluxes (see Section S3 in Supporting Information S1) in favor of molecular diffusion (Ehhalt & Rohrer, 2013; Yonemura, Yokozawa, et al., 2000), the two conductances are:

$$g_\delta = \frac{D_\delta}{\delta}, \qquad g_s = \frac{D_s(\bar{s})}{\ell}, \tag{7}$$

where δ is the depth of the diffusive barrier (litter layer or snow cover), ℓ serves as a diffusive layer length-scale, which field analysis (e.g., Schmitt et al., 2009) suggest to be on the order of one centimeter, $\ell \approx 1$ cm, and D_δ and D_s are the diffusivities. Gas diffusion in soil is greatly influenced by soil physical properties such as texture and structure, conditioning, pore-size distribution, tortuosity and connectivity. A general form of predicting models for gas diffusivity in soil is (Moldrup et al., 2013),

$$\frac{D_s}{D_0} = \alpha_1 n^{\alpha_2} (1 - \bar{s})^{\alpha_3} \tag{8}$$

where D_0 (cm^2/s) is the free air diffusion coefficient (Yonemura, Yokozawa, et al., 2000). α_i are constants that depend on the model adopted and are here defined after Moldrup et al. (1999) as $\alpha_1 = 1$, $\alpha_2 = 2$, and $\alpha_3 = 2 + 3/b$, where b is Campbell's parameter (Campbell, 1974) representing local scale heterogeneity in the soil bulk density (Moldrup et al., 2004)—see Equation 12. Anticipating one of the main conclusions of this work that soil gas diffusivity is one of the controlling processes in H$_2$ uptake, we stress the importance of using a versatile and robust model of soil diffusivity. To this regard, the model used here—also referred to as Buckingham-Burdine-Cambell model—has been verified to be suitable in a variety of undisturbed natural soils (Moldrup et al., 2004). On the contrary, the frequently used model by (Millington & Quirk, 1961)—in which $\alpha_1 = 1$, $\alpha_2 = 4/3$, and $\alpha_3 = 10/3$— has never been validated against gas diffusivity data for undisturbed soils and is instead more suitable for sieved and repacked soils (Moldrup et al., 2004, 2013). Note that Equation 8 is also used to model H$_2$ diffusivity through the litter layer or snow cover—that is, D_δ in Equation 7—by considering $\bar{s} = 0$ and an arbitrary porosity of 0.5 when measurements are not available.

2.3. Biological Sink

Following (Ehhalt & Rohrer, 2013; Schmitt et al., 2009; Yonemura, Yokozawa, et al., 2000), a first order closure is assumed for the depth-averaged consumption of atmospheric H$_2$ by soil bacteria,

$$BD = k\,\bar{\Theta}\,\bar{c}, \tag{9}$$

where k (s^{-1}) is the rate of biological removal, which ideally depends on the amount of H$_2$-oxidizing bacteria within the soil and several abiotic parameters that might affect bacteria metabolism such as the soil type, temperature, soil moisture, organic content, pH, and salinity. We here focus on the sensitivity to temperature and soil moisture, and assume that H$_2$-oxidizing bacteria are spread within the depth Z and are not limited by other abiotic factors (e.g., pH). This hypothesis could be relaxed as further research sheds more light on the links between microbial communities and ecosystem and soil types (Khdhiri et al., 2015). Following the common approach (Ehhalt & Rohrer, 2011; Smith-Downey et al., 2006), we assume that the bacterial metabolism rapidly adapts to soil moisture and temperature as in,

$$k\,\bar{\Theta} = h(T) f(\bar{s}) k_m, \tag{10}$$

where k_m is the decay-rate in non-limited condition, which is assigned a value of 0.03 s^{-1} (e.g., Morfopoulos et al., 2012). This is likely a lower bound estimate as it comes from few laboratory experiments with disturbed (sieved and repacked) soils (Ehhalt & Rohrer, 2011; Smith-Downey et al., 2006) —see Section S4 in Supporting Information S1 for a discussion on different representations of Equation 10. $h(T)$ and $f(\bar{s})$ are normalized functions defined between 0 and 1 that account for possible limitations induced by temperature and soil moisture, respectively, to the H$_2$ biotic consumption. Regarding the influence of temperature, several experimental and field data (collected in Ehhalt & Rohrer, 2011, and shown by gray symbols in Figure 2a) have shown that the biological activity is enhanced by warmer temperatures up to a maximum for T between 30°C and 40°C. The function $h(T)$ is defined through the fit (solid line in Figure 2a) suggested by Ehhalt and Rohrer (2011).

The function $f(\bar{s})$ defines the response of the biotic H$_2$ consumption to soil moisture, and includes both the dependence of bacteria metabolism to water availability and the decay of the air volume fraction at increasing moisture values (see also Section S4 in Supporting Information S1). Laboratory experiments (Conrad & Seiler, 1981; Smith-Downey et al., 2006) have shown that the biological activity is inhibited in very dry soil when bacteria
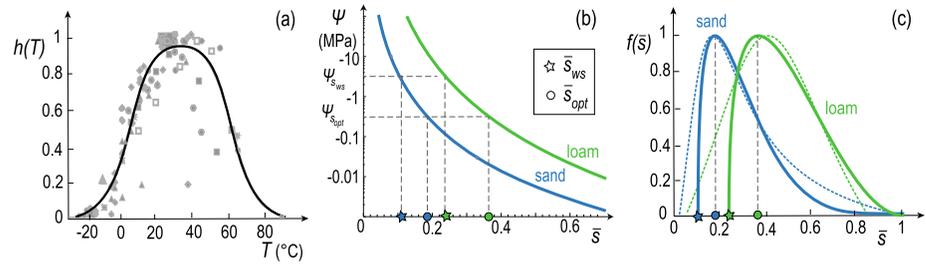
Figure 2. Modeling the H_2 biological sink. (a) Influence of temperature on the bacteria metabolism (adapted from Ehhalt and Rohrer (2011)). (b) Examples of soil water retention curves for sand and loam soils. The curves are used to derive values of the soil water levels for the thresholds $\bar{s}_{ws}$ and $\bar{s}_{opt}$ from $\Psi_{s_{ws}}$ and $\Psi_{s_{opt}}$, respectively. (c) Normalized beta functions (11) for two types of soils. The dotted colored lines are the normalized polynomial fits suggested by Ehhalt and Rohrer (2011).

reversibly enter a metabolically less active state termed dormancy (Leung et al., 2020), and that there is an optimum moisture condition ($\bar{s}_{opt}$) that maximizes the bacteria metabolic rate. At high values of soil moisture, the biological activity may be reduced by other limiting processes (e.g., anoxia). Unfortunately, while these relations between biological activity and soil moisture have been qualitatively observed for several soil types, a quantitative characterization is currently very limited (Ehhalt & Rohrer, 2011). To provide a flexible parametrization adaptable to all soil types, here we model $f(\bar{s})$ using a family of modified beta distributions,

$$f(\bar{s}) = \frac{1}{N}(\bar{s} - \bar{s}_{ws})^{\beta_1}(\bar{s}_{up} - \bar{s})^{\beta_2},\tag{11}$$

where $\bar{s}_{ws}$ and $\bar{s}_{up}$ are the soil-dependent lower and upper moisture threshold for bacterial activity, respectively; and N is a normalization constant such that $\max(f) = 1$. Recent research has shown that low H_2-consumption occurs also in hyper-dry conditions as bacteria harvest trace gas to meet energy demands during starvation (Jordaan et al., 2020; Leung et al., 2020). However, this consumption is three orders of magnitude lower than that occurring during hydration (Jordaan et al., 2020) and can thus be neglected for our purposes ($f = 0$ for $\bar{s} < \bar{s}_{ws}$ and $\bar{s} > \bar{s}_{up}$). Regarding the beta parameters β_1 and β_2, the former is chosen as $\beta_1 = 0.4$ based on a comparison with previous experimental fits (Ehhalt & Rohrer, 2011), while the latter is chosen to impose that the maximum of the beta distribution is at $\bar{s} = \bar{s}_{opt}$, that is, $\beta_2 = \beta_1(1 - \bar{s}_{opt})/(\bar{s}_{opt} - \bar{s}_{ws})$.

To define the soil-dependent values of $\bar{s}_{ws}, \bar{s}_{up}, \bar{s}_{opt}$, we relate the bacterial activity to the soil water potential, which is the best criterion to measure soil water availability to plants and microbial communities (e.g., Brady et al., 2008; King, 2017; Manzoni et al., 2012). The soil matric potential in fact defines the energy state of soil water (relative to the reference potential of zero) in virtue of capillary and adsorptive forces that attract the water to the soil matrix. In analogy to plant stress models (e.g., Porporato et al., 2001), we introduce soil matric potential levels at which bacterial activity is favored ($\Psi_{s_{opt}}$) or inhibited because of water stress ($\Psi_{s_{ws}}$) or anoxia ($\Psi_{s_{up}}$), respectively. In turn, the soil matric potential is related to relative soil moisture by the so-called retention curve (Campbell, 1974; Clapp & Hornberger, 1978),

$$\Psi = \tilde{\Psi}\bar{s}^{-b},\tag{12}$$

where $\tilde{\Psi}$ and b are experimentally determined parameters that depend on soil type (see Table A1 in Appendix A). The soil-water retention curves for sand and loam are reported in Figure 2b. For the values of $\Psi_{s_{opt}}, \Psi_{s_{ws}}, \Psi_{s_{up}}$ we refer to the laboratory results of Smith-Downey et al. (2006); Conrad and Seiler (1981); see Appendix A. We fix $\bar{s}_{up} = 1$, that is, no inhibition of bacteria metabolism for anoxia up to saturation. Figure 2c shows the beta distributions (solid lines) for two different types of soil. The normalized polynomial fits (dotted lines) suggested by (Ehhalt & Rohrer, 2011) for the same soils are also reported, showing lower values for the water-stress threshold $\bar{s}_{ws}$.

Regarding the production of H_2 by nitrogen-fixing bacteria, in most cases the hydrogen thus formed is rapidly consumed either by other bacteria or directly within the cell of the same nitrogen-fixing bacteria that have also developed hydrogenase enzymes to recycle the H_2 (Khdhiri et al., 2017; La Favre & Focht, 1983; Robson & Postgate, 1980). For this reason, we assume $P = 0$ in our simulations. We leave the term P in the theoretical considerations so that, if needed, a production model can readily be implemented.
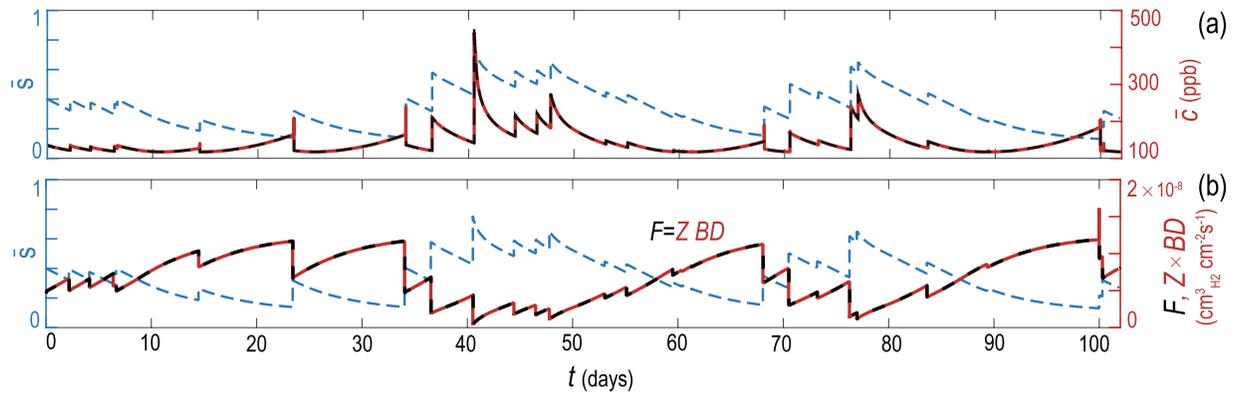
Figure 3. Example of time series for a loamy sand for the depth-averaged soil moisture $\bar{s}$ (dashed blue lines) and the hydrogen related quantities (solid red and dashed black lines): (a) depth-averaged concentration $\bar{c}$ in the soil air; and (b) diffusive flux F (black dashed line) and biological consumption $Z\,BD$ (solid red line). The dashed black line in panel (a) comes from the analytical relationships (13). Parameters of the simulation: $Z = 30$ cm, $\delta = 1$ cm, $\ell = 1$ cm, $\alpha = 1.5$ cm, $\lambda = 0.2$ days^{-1}, $T = 20°$C, and $c_a = 530$ ppbv.

3. Results

3.1. Soil-Moisture Modulation of H$_2$ Dynamics

To focus on the influence of soil-moisture fluctuations on hydrogen dynamics, we here fix the other environmental variables (e.g., the temperature T and the depth of the diffusive barrier δ). Figure 3 shows an example of a time-series from system (3) to (4) for typical growing season and a loamy sand in a temperate climate. For the depth-averaged moisture dynamics of Equation 3, we follow the stochastic approach of (Laio et al., 2001; Yin et al., 2019), where the rain $R(t)$ is in the form of pulses of random depth occurring as a Poisson process with frequency λ (day^{-1}) and events carrying a random depth of rainfall with exponential distribution of mean α (cm) (Rodriguez-Iturbe et al., 1999).

The crucial influence of soil moisture on the H$_2$-related quantities is evident in Figure 3, where we have reported the depth-averaged concentration $\bar{c}$ (first row) and the diffusive flux F and the biological decay $Z\,BD$ (second row). In this example, the soil is sufficiently moist to enable bacterial activity. An increase in soil moisture corresponds to a decrease in the H$_2$ flux F, as a result of the limited diffusivity of hydrogen into the soil.

An important feature shown by Figure 3b is that the diffusive flux F (dashed black line) is in equilibrium with the biological decay $Z\,BD$ (solid red line), that is, $F = Z\,BD$, since the H$_2$ that enters the soil is rapidly consumed by bacteria. From a modeling point of view, this implies that the time derivative in Equation 4 can be neglected, as the hydrogen dynamics is tightly coupled to soil moisture dynamics (Ehhalt & Rohrer, 2013; Yashiro et al., 2011). From $F = Z\,BD$ and using Equations 5 and 9 for the diffusive flux and the biological decay, respectively, one obtains an analytical relationship for the depth-averaged concentration of hydrogen in the soil-air,

$$\bar{c}(t) = \frac{c_a}{1 + v_{BD}/g_T}, \tag{13}$$

where $v_{BD} = Zk\Theta$ is a velocity that indicates the potential of the biological sink along the depth Z. $\bar{c}$ from Equation 13, plotted in Figure 3a (dashed black line), perfectly superimpose on the numerical results obtained without the quasi-steady approximation for the hydrogen dynamics.

3.2. Deposition Velocity: Sensitivity Analysis and Validation

The key quantity for the assessment of the H$_2$ soil sink is the deposition velocity v_d, defined as $v_d = F/c_a$ (e.g., Ehhalt & Rohrer, 2009). An analytical relationship for v_d can be obtained substituting the equilibrium relationship (13) for $\bar{c}$ into the diffusive flux (5), obtaining:

$$v_d(t) = \frac{g_T\, v_{BD}}{g_T + v_{BD}}. \tag{14}$$
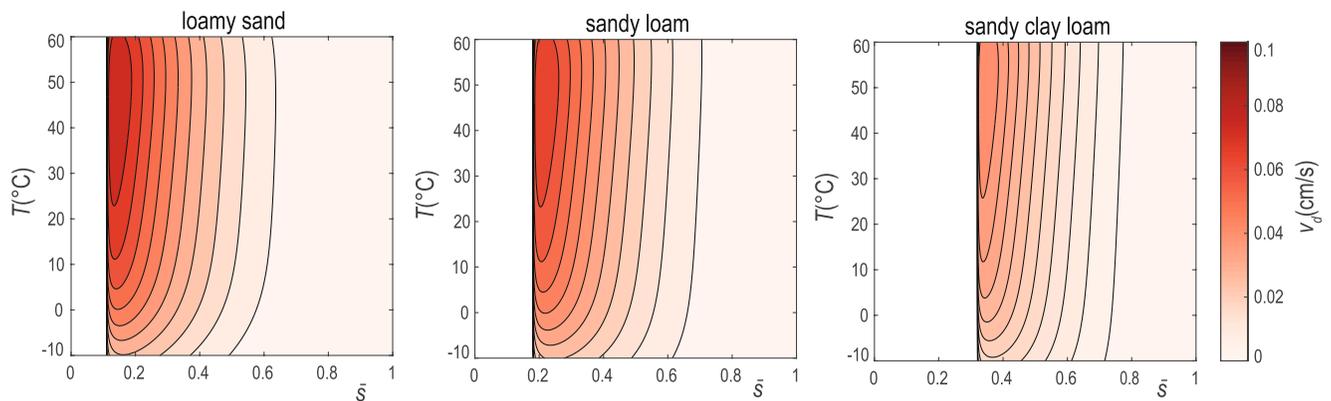
Figure 4. Sensitivity of the deposition velocity v_d from Equation 14 to temperature T and soil moisture $\bar{s}$ for three different soils ($\delta = 0$ cm, $\ell = 1$ cm, and $Z = 15$ cm).

A comparison between this novel analytical relationship and the notable model by Ehhalt and Rohrer (2013) is reported in Appendix B. The analytical expressions for $\bar{c}$ and v_d that account for the production term P are reported in Appendix C.

The deposition velocity v_d is shown as a function of soil moisture and temperature for different soil types in Figure 4. For soil moisture values below the soil-dependent water-stress threshold ($\bar{s} < \bar{s}_{ws}$), there is no soil H_2 uptake ($v_d = 0$). For soil moisture values that are slightly above $\bar{s}_{ws}$, the active biotic metabolism and the favorable conditions of H_2 diffusion through the soil determine a maximum for the deposition velocity. As soil moisture increases, the deposition velocity decays due to the limited H_2 diffusivity through the soil. Warm temperatures ($T > 25°C$) enhance the bacterial metabolic rate and define maximum conditions of H_2 uptake.

To validate the relationship (14), we use measurements collected continuously over a year, from December 2010 through February 2012, at the Harvard Forest (Meredith, 2016). This is a temperate mixed deciduous forest, characterized by a sandy loam glacial till with relatively high levels of total carbon and nitrogen and high-affinity hydrogenase (Meredith et al., 2017). The data set is one of the most extensive soil-atmosphere flux measurements of hydrogen to date and notably includes the temporal variations of the hydro-climatic forcing (temperature, rain, snow cover depth and porosity) that are necessary for a field-theory comparison. These besides snow porosity are shown in Figure 5a.
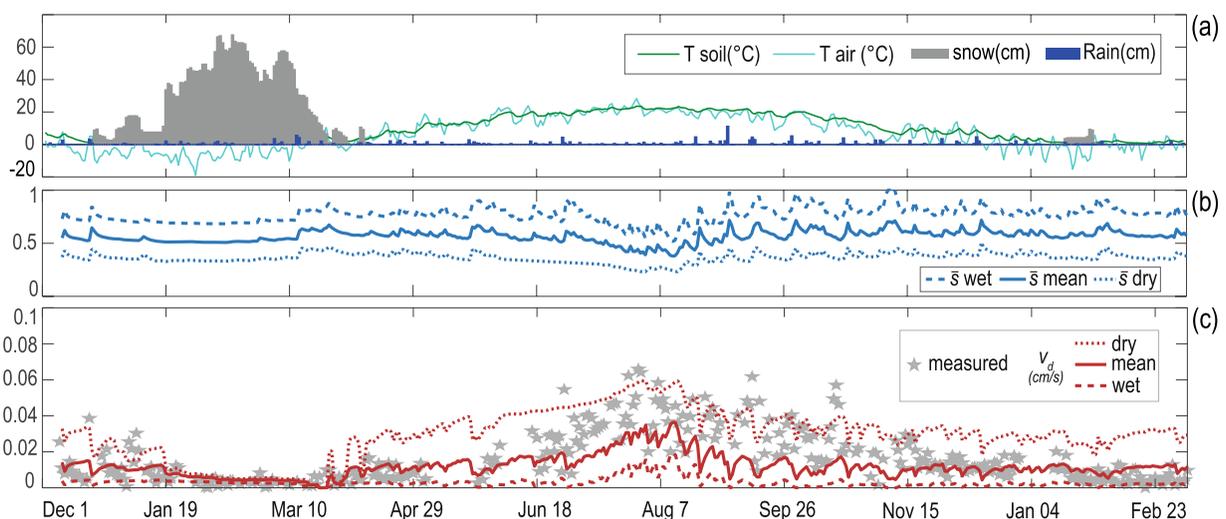
Figure 5. Hydroclimatic forcings and H_2 uptake at the Harvard Forest from December 2010 through February 2012. Measured data are from Meredith (2016) and Meredith et al. (2017). (a) Measured rain, snow cover, and soil and air temperatures. (b) Values of soil moisture measured at two locations in the Harvard forest ($\bar{s}_{dry}$ for the well-drained location and $\bar{s}_{wet}$ for the poorly drained location). $\bar{s}_{mean}$ shows the mean values between the two locations. (c) Modeled deposition velocity v_d ($Z = 15$ cm).
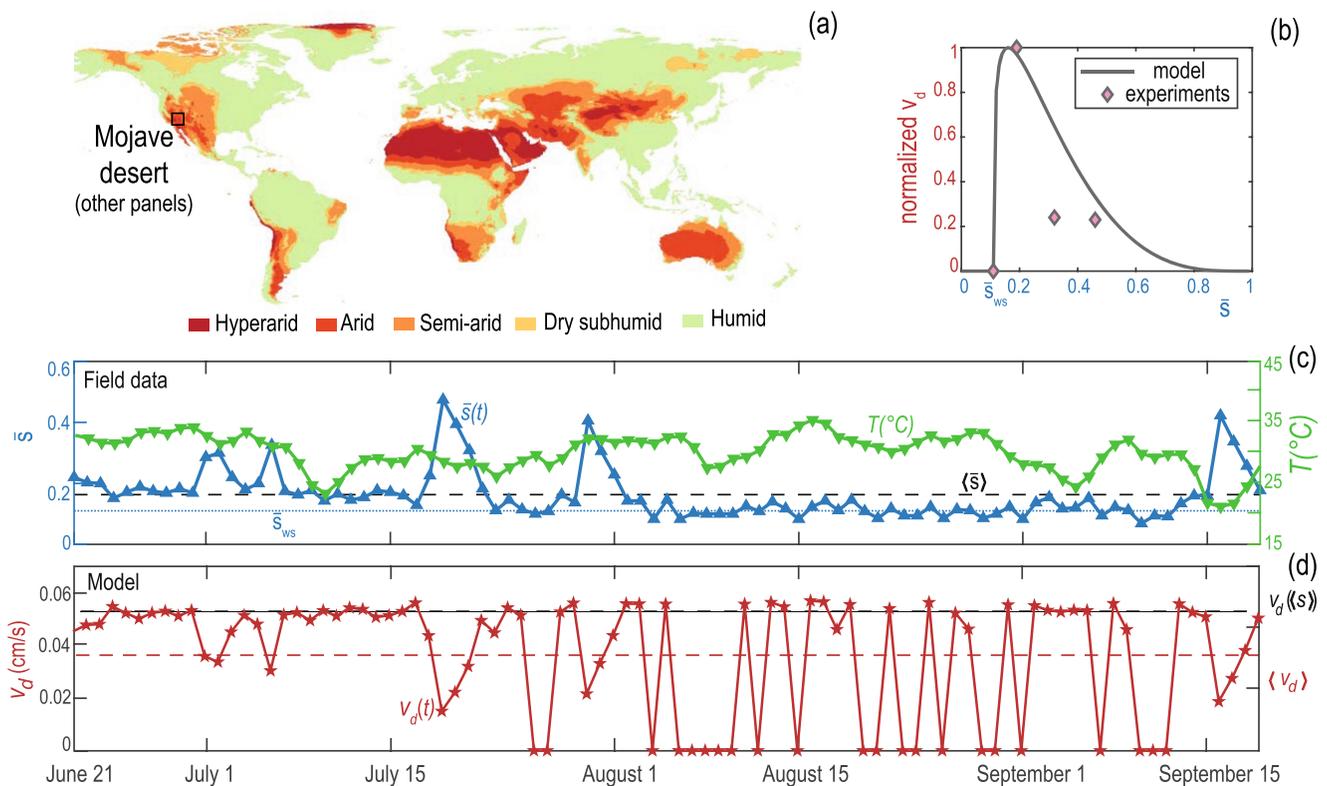
Figure 6. Example of intermittent H_2 uptake driven by soil moisture fluctuations around the water-stress threshold for bacteria metabolism. (a) World aridity map (FAO, 2009). (b) H_2 uptake versus the depth-averaged soil moisture $\bar{s}$ for the sand of the Mojave desert. Symbols are from Smith-Downey et al. (2006). (c) Time-series of the hydro-climatic forcings measured at the Mojave desert in the summer of 2015 (data from Larson et al. (2008) and PBO (2020)). The dotted blue line indicates the water-stress threshold $\bar{s}_{ws}$. The dashed black line indicates the time-averaged soil moisture $\langle \bar{s} \rangle$. (d) Intermittent deposition velocity v_d (cm/s) ($Z = 10$ cm).

Regarding the soil moisture values, measurements averaged on the first 15 cm of soil were taken from two locations nearby the H_2 fluxes measurements. One location was well drained ($\bar{s}$−dry in Figure 5b) and the other one was poorly drained ($\bar{s}$−wet). To span the range of possible moisture values in the location of measurement of the hydrogen flux, we evaluate v_d including the soil moisture values from both locations as well as averaged values of soil moisture ($\bar{s}$−mean).

Results for v_d from Equation 14 are compared with field measurements in Figure 5c. The modeled range of deposition velocities captures well the measured temporal trend. Diffusive limitations such as the soil water saturation and the snow cover strongly affect the hydrogen uptake rates. For example, the model reproduces accurately the inhibition of H_2 uptake caused the thick snow cover during the winter 2010–2011. The higher uptake rate during the summer period, with lower level of soil moisture and higher temperatures, is also well predicted. The figure also shows the strong sensitivity of the deposition velocity to the local conditions of soil moisture. From the two measurements of $\bar{s}$ ($\bar{s}$-wet and $\bar{s}$-dry), the calculated deposition velocities show a remarkable difference (besides during the winter 2011 when the thick snow cover inhibits the H_2 uptake regardless of the underlying moisture value). This underlines that local soil conditions may generally cause marked spatial patterns of hydrogen uptake even within the same ecosystem, especially in the presence of complex topography (e.g., ridges and valleys). This should be carefully considered when deriving a deposition velocity from field measurements at a point or when space-averages of soil moisture are used for global assessments of hydrogen uptake.

3.3. The Intermittency of H_2 Soil Uptake

To uptake H_2, the soil has to be sufficiently moist to enable the metabolism of the H_2-oxidizing bacteria (Conrad & Seiler, 1981; Smith-Downey et al., 2006). As bacteria remain active down to low moisture levels, the biotic inhibition due to water-stress only occurs in dry soils (Figure 6a). Here, bacteria can face prolonged and severe water stress, which curtails cellular and metabolic activities, until transient water availability—caused for instance
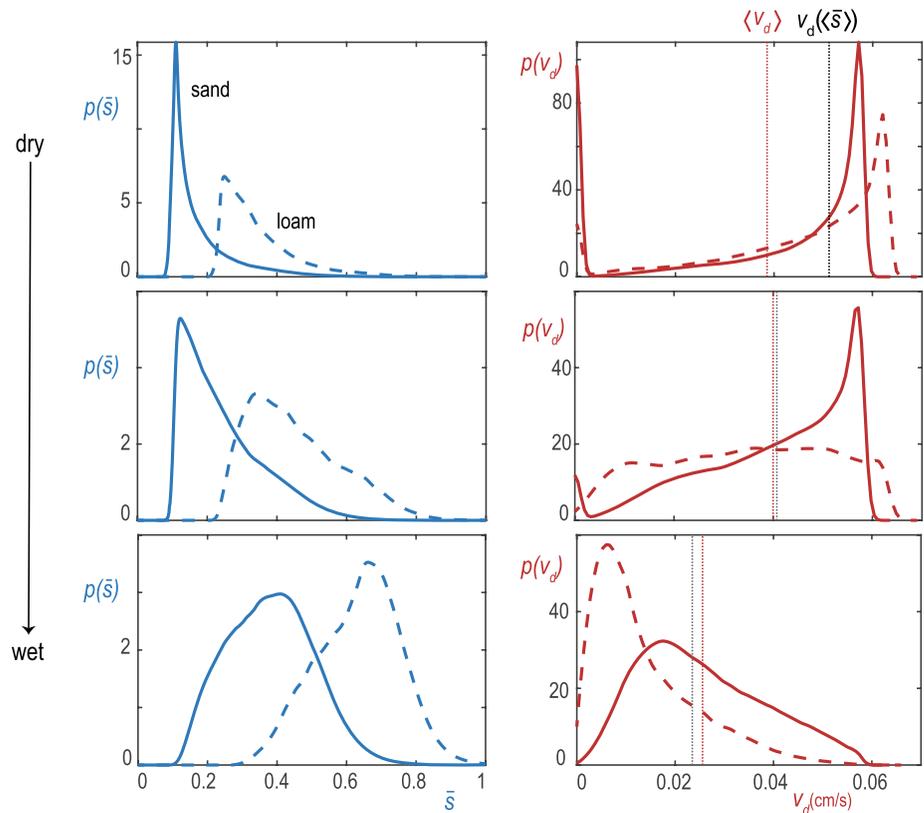
Figure 7. Probability density functions of soil moisture $\bar{s}$ (first column) and deposition velocity v_d (second column) for different types of soil and mean rainfall rate. Solid lines are for a sandy soil and dashed lines for a loamy soil. $\langle v_d \rangle$ and $v_d(\langle \bar{s} \rangle)$ are reported for the sand case. Top, center, and bottom graphs have a mean rainfall rate λ of 0.1, 0.2, and 0.5 days^{-1}, respectively. Common parameters to all graphs are: $Z = 30$ cm, $\ell = 1$ cm, $\delta = 0$ cm, $\alpha = 1.5$ cm, and $T = 20°C$.

by dew condensation or an occasional rain event—allow them to generate biomass and accumulate reserve compounds (Leung et al., 2020). Hence, even small fluctuations of soil moisture around the water-stress threshold ($\bar{s}_{ws}$) may amplify the H$_2$ uptake from 0% to 100% of its potential, that is, from the water-stress inhibition to the active bacteria metabolism in condition of fastest H$_2$ diffusion through the soil.

The striking consequences of this effect can be appreciated in the following example. In Figure 6b, the modelled H$_2$ uptake as a function of soil moisture is reported together with the experimental results by Smith-Downey et al. (2006) for the Mojave-desert sand. Using the time-series of measured hydro-climatic variables in the summer 2015 (Figure 6c), the modeled deposition velocity $v_d(t)$ (Figure 6d) exhibits an intermittent trend in the months of August and September as a result of the moisture fluctuations around the water-stress threshold $\bar{s}_{ws}$. As a consequence, a strong difference between the true averaged deposition velocity, $\langle v_d \rangle$, and the deposition velocity obtained through the averaged soil moisture value, $v_d(\langle \bar{s} \rangle)$, is observed, with an error around 35%. As dry regions represent about 1/3 of global land (Figure 6a), this intermittent feature of H$_2$ uptake highlights a delicate aspect for estimating the magnitude and spatial distribution of H$_2$ removal using global models (as further discussed in Section 4.1).

3.4. Probabilistic Dynamics

Because on long timescales rainfall acts as a random forcing of the moisture and hydrogen dynamics, it is useful to investigate the solution to the system (3)–(4) in terms of probability density function (pdf) of moisture and hydrogen uptake. This analysis helps address stochastic conditions of hydrogen uptake as a function of the frequency and intensity of the rainfall regime. From the soil moisture pdf, obtained following (Laio et al., 2001; Yin et al., 2019), the pdf of the deposition velocity v_d is obtained as a derived distribution (Benjamin & Cornell, 2014) using Equation 14. Figure 7 shows some examples of pdf's of soil moisture (first column) and deposition velocity
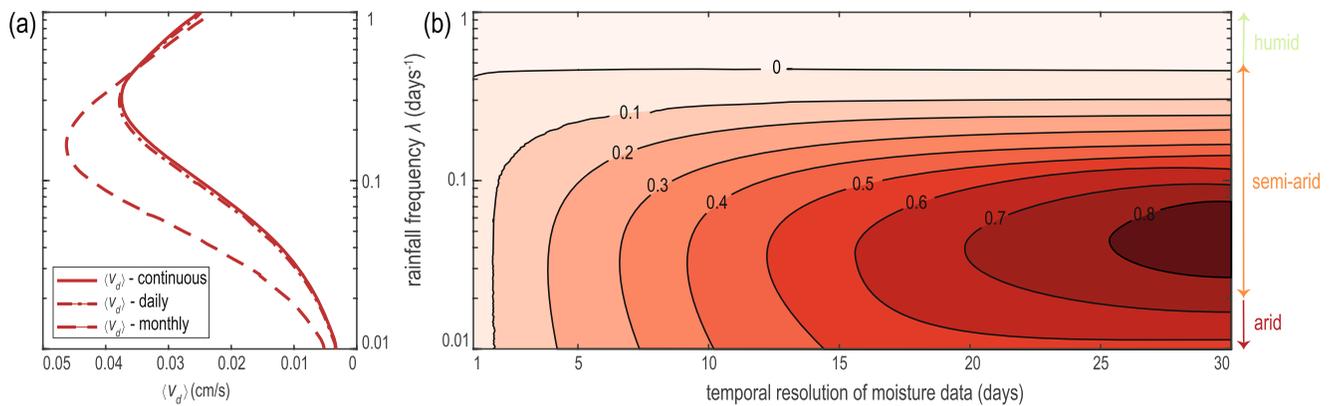
Figure 8. Effect of the rainfall regime and the temporal resolution of soil moisture data on the estimate of the soil H_2 uptake. (a) Average deposition velocity $\langle v_d \rangle$—from continuous, daily averaged, monthly averaged soil moisture values—as a function of the rainfall frequency (constant average depth of the rainfall event $\alpha = 1$ cm). (b) Relative error on the deposition velocity due to the temporal resolution of the soil moisture data (sand soil, $Z = 15$ cm, $\delta = 0$, and $T = 20°C$).

(second column) for two types of soil (sand and loam) for different rainfall frequencies. The moisture pdf's are shifted toward lower values for the soil with the coarser texture (sand). The shape of the moisture pdf's undergoes marked changes with the rainfall frequency, with the sharpest pdf's corresponding to dry soils.

In dry climates (upper panels), the pdf's of v_d show a strong bimodality (in particular for the sand example), where the two modes correspond to no deposition and maximum deposition, respectively. The bimodality arises from the fluctuations of soil moisture around the water-stress threshold, which control the switch from a maximum uptake of H_2 to no uptake on daily timescales (see previous section). Addressing this temporal dynamics is necessary to correctly quantify the H_2 soil uptake as the sole knowledge of the time-averaged soil moisture $\langle \bar{s} \rangle$ is insufficient—see the difference between $v_d(\langle \bar{s} \rangle)$ and $\langle v_d \rangle$.

In wetter climates, as soil moisture is maintained above the water stress threshold for hydrogen consumption, the pdf's of v_d tend to lose the bimodality and become flatter. In such conditions, soil texture plays an important role as it influences, in addition to the soil moisture dynamic, the diffusion of H_2 through the soil. Coarser soils favor hydrogen uptake through an increased diffusivity. As soil moisture approaches saturation, hydrogen uptake is inhibited by the limited diffusion (see the dashed lines in the lower row of panels). This latter condition might be representative, for example, of wetlands. Because in wetter climates soil moisture fluctuates in the quasi-linear decreasing branch of $v_d(\bar{s})$, the time-average soil moisture $\langle \bar{s} \rangle$ is sufficient to characterize the average conditions of soil H_2 uptake ($v_d(\langle \bar{s} \rangle) \sim \langle v_d \rangle$).

4. Discussion

In this section, we discuss the global implications that the soil dry-wet sequences (Section 4.1), the abiotic-biotic limitations (Section 4.2), and the changing climate (Section 4.3) have on the soil H_2 sink.

4.1. Control of Dry-Wet Sequences in Semi-Arid Regions

Because the H_2 uptake is nonlinearly driven by the soil moisture dynamics, the temporal resolution of the soil moisture data is a key aspect for a correct evaluation of the soil H_2 sink (Sections 3.3–3.4).

As an example, Figure 8 shows the time-averaged deposition velocity $\langle v_d \rangle$ for a sand soil as a function of the temporal resolution of soil moisture data and the intensity of the rainfall regime. The latter is represented in terms of changes in rainfall frequency λ (log-scale), while the mean rainfall depth α is kept constant. The deposition velocity obtained from daily averaged soil moisture data, $\langle v_d \rangle$-daily, well reproduces the average deposition velocity obtained from a continuous series of soil moisture through Equation 3, $\langle v_d \rangle$-continuous, while the deposition velocity obtained from monthly averaged soil moisture data, $\langle v_d \rangle$-monthly, is biased toward higher values (Figure 8a). The relative error on $\langle v_d \rangle$ increases monotonically with the temporal resolution of the moisture data and
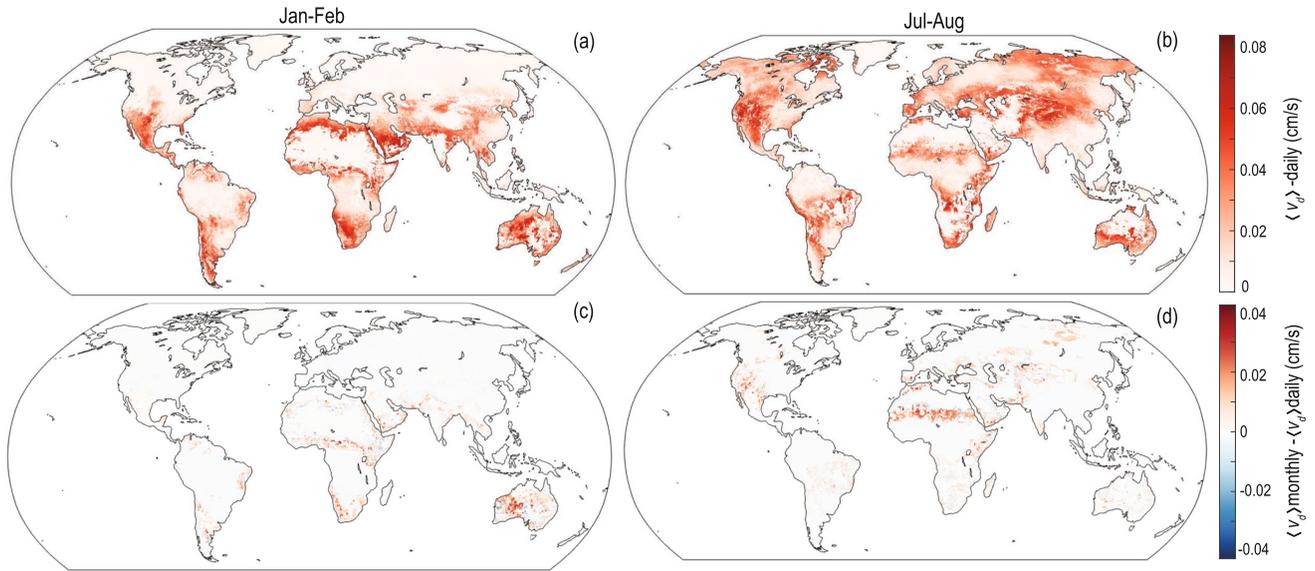
Figure 9. Effect of seasonality and the temporal resolution of the hydroclimatic data on the global distribution of soil H_2 uptake ($Z = 10$ cm). (a and b) Average deposition velocity $\langle v_d \rangle$ from daily averaged Global Land Data Assimilation System data of 2019. (c and d) Differences in $\langle v_d \rangle$ caused by monthly averaged data.

shows a maximum for semi-arid climates (Figure 8b), wherein the temporal fluctuations of soil moisture around the water-stress threshold may define the intermittent dynamics of the soil H_2 uptake (see Section 3.3).

Using daily hydroclimatic and soil data with spatial resolution of 15 arc min—nearly 28×28 km at the equator—from the Global Land Data Assimilation System (Rodell et al., 2004), we evaluated the global distribution of the average deposition velocity $\langle v_d \rangle$ during the summer and winter months of 2019 (Figures 9a and 9b). The regions that maximize the H_2 uptake are those sufficiently moist to enable the bacteria activity, but sufficiently dry to favor gas diffusion through the soils, that is, dry sub-humid and semi-dry regions (see also the World aridity map in Figure 6a). Conversely, very dry (e.g., Sahara desert) or wet (e.g., tropical forests) regions are characterized by no uptake and low uptake, respectively, although the limiting processes are different (as further discussed in the next section). These global trends well reproduce the recent results in Paulot et al. (2021), but did not require ad hoc corrections to the soil moisture data nor the introduction of a carbon-based function to mask the H_2 uptake in arid regions.

The difference in the global distribution of $\langle v_d \rangle$ caused by monthly averaged data is shown in Figures 9c and 9d. The greatest differences are obtained in the regions where the H_2 uptake is likely favored (semi-dry regions), as here the H_2 uptake is very sensitive to soil moisture and its temporal fluctuations around the water-stress threshold for bacteria metabolism.

We stress that similar issues, that is, large errors in the estimate of the H_2 uptake due to averaged moisture data, may also occur when using space-averaged soil moisture data in regions characterized by a complex topography and strong spatial patterns of soil moisture and, consequently, H_2 uptake. Accounting for spatial heterogeneity at the sub-grid scale could help address this problem in global climate models (e.g., Chaney et al., 2018; Paulot et al., 2018).

4.2. Biotic and Abiotic Limitations of H_2 Uptake

The relationships (13) and (14) for the depth-averaged H_2 concentration $\bar{c}$ and the deposition velocity v_d allow us to neatly assess the relative extent of biotic and abiotic limitations in the soil H_2 uptake. Two terms are involved: the total conductance, g_T (cm/s), which is a function of hydrogen diffusivity through the soil and possible diffusive barriers, and v_{BD} (cm/s), which is the potential hydrogen consumption by bacteria along the soil depth Z. To understand which process may be limiting the H_2 uptake, it is useful to note that $2v_d$ corresponds to the harmonic mean between biological (v_{BD}) and diffusive (g_T) velocities; hence, by comparing the magnitude of the two terms, one can easily draw the distinction,
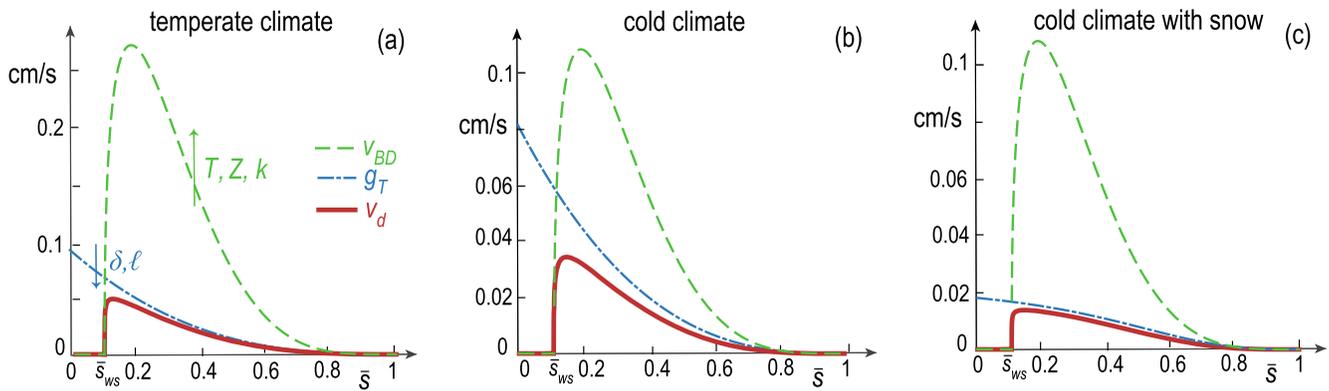
Figure 10. Deposition velocity v_d as a balance between diffusive (g_T) and biological (v_{BD}) processes (sand soil, $Z = 10$ cm). (a) $T = 20°C$ and $\delta = 0$. (b) $T = 0°C$ and $\delta = 0$. (c) $T = 0°C$ and $\delta = 10$ cm. Note the different scales on the y axes.

$$v_d \sim \begin{cases} g_T & \text{if } v_{BD} \gg g_T \quad \text{(diffusion limited)}, \\ v_{BD} & \text{if } g_T \gg v_{BD} \quad \text{(biotic limited)}. \end{cases} \tag{15}$$

Equivalently, Equation 13 states that $\bar{c} \ll c_a$ in diffusive limited condition and $\bar{c} \sim c_a$ in biologically limited conditions.

Figure 10 shows a graphical comparison between g_T and v_{BD} as a function of soil moisture for a sandy soil in temperate and cold climates. No diffusive barrier is included besides for the snow case (panel c). For low values of soil moisture ($\bar{s} < \bar{s}_{ws}$), the lack of water inhibits the bacterial metabolism and hence the H_2 soil uptake is biologically limited ($v_d = v_{BD} = 0$). Globally (Figure 11), biotic limitations due to water-stress characterize arid and hyperarid regions (e.g., Sahara desert) and the dry season of zones with tropical savanna climate (e.g., Brazil Cerrado).

For higher values of soil moisture ($\bar{s} > \bar{s}_{ws}$), diffusion generally limits the H_2 uptake in temperate climate (Figure 10a), that is, the biotic consumption is limited by the little amount of substrate available. This is consistent with previous field observations (e.g., Schmitt et al., 2009; Smith-Downey et al., 2008) that measured a complete H_2 decay within the first centimeters (e.g., 1–5) of soil in favorable metabolic conditions. The diffusive limitation would be even more evident in the presence of a diffusive barrier (g_T decreases with δ), with a different soil type (sand favors gas diffusion), with a warmer climate (the temperature T mainly boosts the potential biological consumption v_{BD}) and with a higher Z (the depth of soil wherein H_2-oxidizing bacteria are present). Regarding the latter, we have in fact used a conservative hypothesis that H_2-oxidizing bacteria are found just within the first 10 cm of soil, while recent microbial analyses (Bay et al., 2021) have revealed their presence along the first 30 cm of soil in several ecosystems worldwide, that is, v_{BD} could be much higher. For these reasons, we find that globally diffusion limits the H_2 uptake in all temperate and tropical humid regions, as well as zones with tropical savanna climate during the wet season (Figure 11). It is worth noticing that, when $v_d \sim g_T$, the uncertainties in the parametrization of the biological metabolism might be conveniently avoided.

In cold humid climates, as the bacteria metabolism is hindered by low temperatures, v_{BD} and g_T are comparable and both biotic and abiotic factors concur in determining a low deposition velocity (Figure 10b). However, in the presence of a snow cover, the H_2 soil uptake newly becomes a diffusion-limited process (Figure 10c). Overall, these results indicate that H_2 soil uptake is a diffusive-limited process, besides in very dry or cold soils. Note that this conclusion is basically independent of the functional form for the biological decay (see Section S5 and Figure S2 in Supporting Information S1).

As the soil approaches saturation, the H_2 uptake is inhibited (Figure 10). Understanding whether this is mainly due to reduced diffusivity or the reduced biological metabolism partially remains an open challenge. From a modeling perspective, this would require defining which term (g_T or v_{BD}) decays to zero more rapidly as the soil approaches saturation. Because of our parametrization of v_{BD}, which depending on the type of soil might have
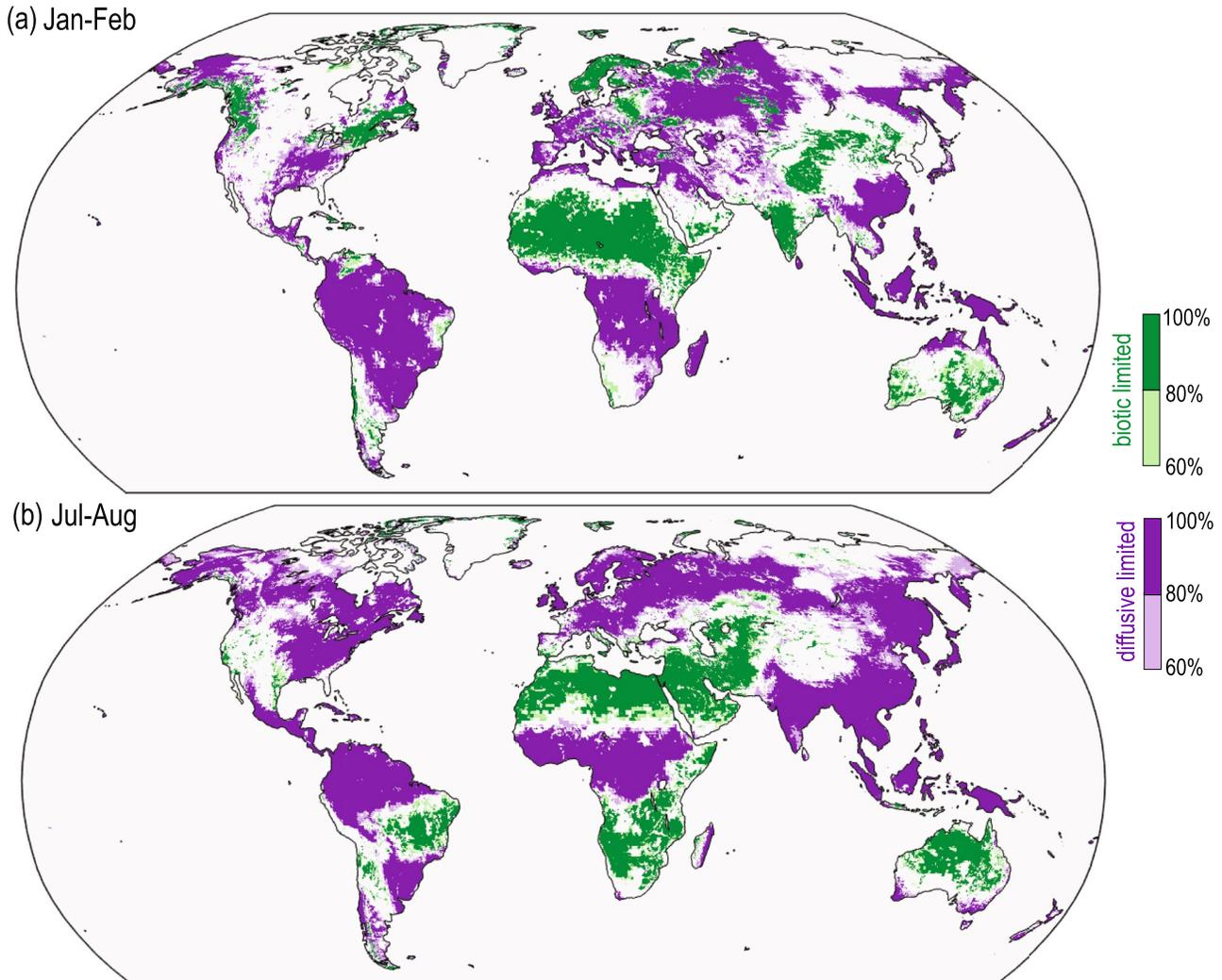
Figure 11. Global distribution of the relative frequency of diffusive and biotic limitations to soil H_2 uptake for the nominal year 2019 ($Z = 10$ cm). Diffusive (biotic) limited when $v_{BD} > 6\, g_T$ ($g_T > 6\, v_{BD}$) and $0.85 < v_d/g_T < 1.15$ ($0.85 < v_d/v_{BD} < 1.15$).

a weak or strong decay at increasing $\bar{s}$ (see Figure 2c), we find soil-dependent limitations (e.g., biological for a sand and diffusive for a loam). A linear parametrization for v_{BD} (see Section S5 and Figure S2 in Supporting Information S1) provide diffusive limitations for all soils. Experiments in conditions close to water saturation could probably address this question as, if diffusion is limiting, $\bar{c} \ll c_a$, while, if biotic metabolism is limiting, $\bar{c} \sim c_a$.

4.3. Perspective

Distinguishing between diffusive and biological limitations is an important step forward in the understanding of the processes controlling the H_2 uptake and its relations to the hydroclimatic forcings. For this reason, it is useful to discuss future implications that an increased use of hydrogen for energy production may have on the global soil H_2 uptake within the context of a changing climate.

The globally widespread diffusive limitation (Figure 11) suggests that there is a higher potential of H_2 uptake by bacteria. This is in agreement with the saturation mixing ratio for microbial H_2 consumption being much higher than current atmospheric levels (Greening et al., 2015; Schmitt et al., 2009). An important modeling consequence is that the first order closure for the H_2 uptake ($F = v_d c_a$) would still be valid for a higher H_2 tropospheric concentration c_a caused, for example, by the transition toward a hydrogen-based economy.
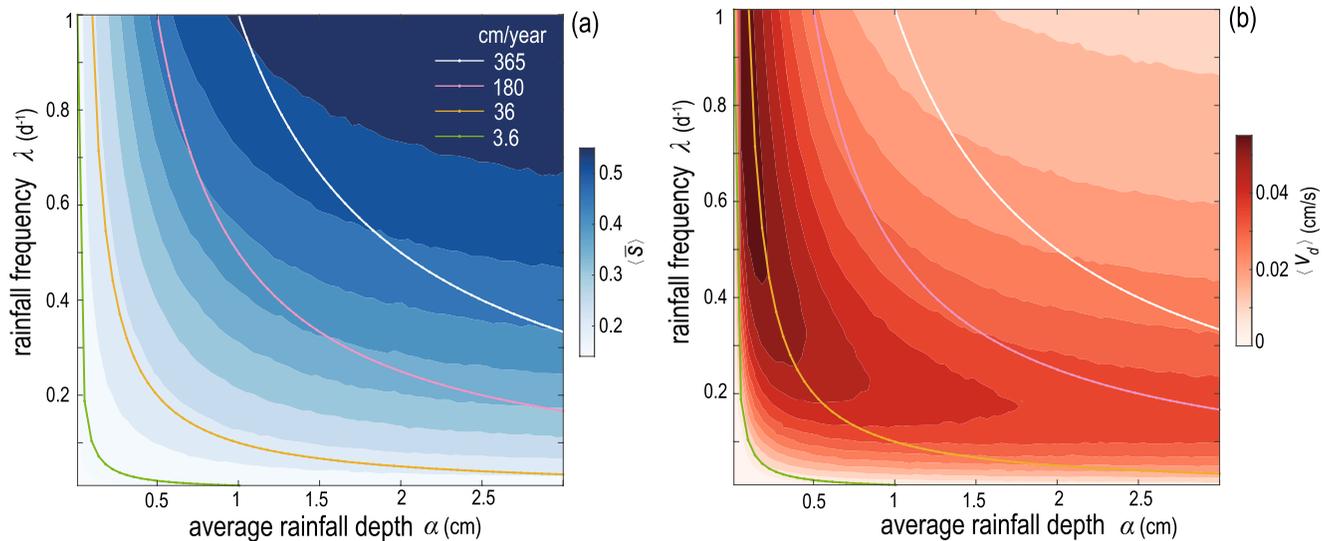
Figure 12. Contour plots of the average soil moisture $\langle \bar{s} \rangle$ (a) and deposition velocity v_d (b) as a function of the average rainfall depth α and frequency λ (loamy sand, $Z = 15$ cm). Solid colored lines define curves with constant accumulated rainfall.

The diffusive and biotic limitations that define the deposition velocity v_d may be affected by variations in the hydroclimatic forcings due to climate change. The globally rising temperatures are slightly favoring both the bacteria metabolism (see Figure 2a) and the H_2 diffusivity. However, because v_d is not very sensitive to small temperature variations (Figure 4), a limited increase in the global average of the deposition velocity can be expected (Paulot et al., 2021).

The response of v_d to variations in the hydrological regime is more complicated to predict, because of the strong underlying nonlinearities and the very diverse changes in rainfall patterns that are being observed at local and regional scales (Feng et al., 2013; Fischer et al., 2014). The analysis is further complicated by the fact that the H_2 uptake is a function of not only the total amount of rainfall, but also of how the rain events are distributed in time. This is highlighted in Figure 12, where the average soil moisture (a) and deposition velocity (b) are evaluated as a function of the average rainfall depth and frequency. In the assumption that, the total amount of rain varies little, but is concentrated in fewer and more intense events (Fischer et al., 2014), a shift toward the right along the solid lines in Figure 12 could be observed. As a result, the H_2 uptake could either increase or decrease, depending on the local hydrological conditions and their climate-change alterations. For example, the lower rainfall frequency could enhance the uptake in humid regions due to longer periods of favored H_2 diffusion, and instead reduce the uptake in semi-dry regions due to longer periods of water-stress biotic limitation (Figure 12b). At the current stage of research, it is unknown whether these local variations of H_2 uptake would compensate on a global level so that no net-effect in the global uptake would be observed.

Finally, it is likely that the presence H_2-oxidizing bacteria will remain widespread in the future due to their adaptability to extreme environments (Ji et al., 2017). However, their spatial heterogeneity may change as a result of climate and anthropogenic pressures.

5. Summary and Conclusion

This paper presents a unified model for the coupled water and hydrogen dynamics in soils, which explicitly accounts for the effects of intermittent soil moisture fluctuations. The hydrogen dynamics consider the diffusive flux between the atmosphere and the soil (Section 2.2) and the biological consumption within the first layers of soil (Section 2.3). As a first main result, we verified from the temporal solutions of the coupled system (Figure 3) that the H_2 dynamics rapidly adapts to the soil moisture conditions. This allowed us to obtain direct relationships for the depth-averaged concentration of H_2 into the soil ($\bar{c}$) and the deposition velocity (v_d)—Equations 13 and 14, respectively. The latter has been shown to reproduce well the time-series of H_2 uptake measured continuously over a year in a temperate forest (Figure 5).

Due to the strongly nonlinear relationship between deposition velocity v_d and soil moisture $\bar{s}$ (Figure 4), when soil moisture fluctuates around the threshold demarcating the water-stress condition for bacteria metabolism, the H_2 uptake may exhibit large temporal variations and intermittency (Figure 6). In these cases, which are representative of semi-arid regions, addressing the fine-scale (e.g., daily) temporal dynamics of soil moisture is crucial to correctly quantify the H_2 uptake (Figure 8).

The analytical relations (13)–(14) further enable the comparison of the relative extent of biotic and abiotic limitations in the H_2 soil uptake as a function of the hydro-climatic variables (Section 4.2). The results (Figure 11) show that H_2 soil uptake is generally a diffusion-limited process in humid temperate and tropical regions, while biological limitations may occur in very dry soils, where the bacterial activity is inhibited by the lack of water, and in cold environments, where the bacterial activity is slowed by the low temperatures. Even in cold regions however, the presence of snow may reduce the diffusivity of H_2 from the atmosphere to the soils up to the point that the hydrogen soil uptake is still a diffusion-limited process (Figure 10c). The overall importance of diffusive limitations suggests that macroporosity may substantially contribute to the H_2 uptake by favoring H_2 diffusion through the soil, an aspect that still needs to be investigated.

The present modeling framework would benefit from further experimental and field research that more precisely characterizes the water-stress threshold for H_2-oxidizing bacteria ($\bar{s}_{ws}$) in terms of water potential, and in relation to the soil and ecosystem characteristics. This threshold in fact is crucial to both discriminate between diffusive and biological limitations in the H_2 soil uptake and define the regions where bacteria transiently suffer water-stress, and where it is thus necessary to consider the temporal fluctuations of soil moisture to correctly evaluate the H_2 soil sink. Additional microbial field analyses could also be useful to depict the vertical distribution of H_2-oxidizing bacteria in soils as well as the temporal dynamics of their metabolism in relation to water availability in semi-arid and arid regions.

Appendix A: Linking Bacterial Metabolism and Soil Matric Potential

We characterize the function $f(\bar{s})$ in Equation 11 in terms of soil matric potential ($\Psi_{s_{opt}}$, $\Psi_{s_{ws}}$, and $\Psi_{s_{up}}$) by referring to the laboratory results of Conrad and Seiler (1981) and Smith-Downey et al. (2006). For the inhibition of bacterial activity due to water stress, the experiments with sand by Smith-Downey et al. (2006) highlighted that, over a broad range of temperatures, biological activity was absent at $\bar{s} \sim 0.11$, which corresponds to $\Psi \sim -2.6$ MPa through Equation 12 and the parameters reported in Table A1. Based on this, and in analogy with the common values for the wilting point of plants in semiarid environments, that is, the condition at which plants stop to transpire (Laio et al., 2001), we take $\Psi_{s_{ws}} \sim -3$ MPa. Regarding the upper limit, as most of the experimental results (Conrad & Seiler, 1981; Smith-Downey et al., 2006) show no biological inhibition until saturation, we fix $\bar{s}_{up} = 1$. For the optimum condition, averaging some experimental soil moisture optima (Conrad & Seiler, 1981; Smith-Downey et al., 2006), we roughly obtain $\Psi_{s_{opt}} \sim -0.3$ MPa. In the following table, we report the corresponding values of soil moisture for different soil types that are obtained from the water retention curves (12) imposing $\Psi_{s_{ws}} = -3$ and $\Psi_{s_{opt}} = -0.3$ MPa.

Table A1
Parameters Describing Various Soil Characteristics Used in the Model for Different Soil Textures

	$\tilde{\Psi}^a$(kPa)	b^a	n^b	$\bar{s}_{ws}$	$\bar{s}_{opt}$
Sand	−0.34	4.05	0.35	0.11	0.19
Loamy sand	−0.17	4.38	0.42	0.11	0.18
Sandy loam	−0.71	4.9	0.43	0.18	0.29
Silt loam	−5.6	5.3	0.47	0.31	0.47
Silt[c]	−5.6	5.3	0.47	0.31	0.47
Loam	−1.4	5.4	0.45	0.24	0.37
Sandy clay loam	−0.85	7.12	0.4	0.32	0.44
Silty clay loam	−1.4	7.75	0.46	0.37	0.50
Clay loam	−3.5	8.52	0.47	0.45	0.59
Sandy clay	−0.6	10.4	0.4	0.44	0.55

Table A1
Continued

	$\tilde{\Psi}^{a}$(kPa)	b^{a}	n^{b}	$\bar{s}_{ws}$	$\bar{s}_{opt}$
Silty clay	−1.7	10.4	0.47	0.48	0.61
Clay	−1.8	11.4	0.5	0.53	0.64

Note. The values of $\bar{s}_{ws}$ and $\bar{s}_{opt}$ have been calculated supposing a soil water potential $\Psi_{s_{ws}} = -3$ and $\Psi_{s_{opt}} = -0.3$ MPa, respectively.

[a]From Clapp and Hornberger (1978). [b]Typical values of soil porosity from Dingman (2015). [c]Same values as silt loam are used.

Appendix B: Comparison With v_d From Ehhalt and Rohrer (2013)

From a two-layer soil model first proposed by Yonemura, Yokozawa, et al. (2000) and Ehhalt and Rohrer (2013) solved the soil H_2 concentration Equation 1 in the vertical direction and derived the following analytical expression for the deposition velocity,

$$v_{d,\text{Ehhalt}} = \frac{g_\delta \sqrt{D_s \Theta k}}{\sqrt{D_s \Theta k} + g_\delta}. \tag{B1}$$

The equation shows that $v_{d,\text{Ehhalt}}$ is half the harmonic mean between the conductance of the diffusive barrier (g_δ) and the velocity ($\sqrt{D_s \Theta k}$), which couples diffusion and biological consumption within the active layer of soil. Hence, for example, in the presence of a diffusive barrier, $g_\delta \ll \sqrt{D_s \Theta k}$, the deposition velocity reduces to $v_d \approx g_\delta$.

Figure B1 shows a graphical comparison between v_d from the depth-averaged model—Equation 14—and the vertically explicit model—Equation B1—versus soil moisture $\bar{s}$ for three different soils. The models provide similar results, besides a difference in the peak value of v_d, which is higher in the depth-averaged model (14). Overall, the main difference between the two models is that, in the depth-averaged approach, diffusive and biotic processes are mathematically separated. This facilitates the comparison between abiotic and biotic limitations in the soil H_2 uptake (as discussed in Section 4.2), but requires the definition of the length-scales Z–related to the vertical distribution of H_2 oxidizing bacteria and ℓ–the diffusive layer length-scale.
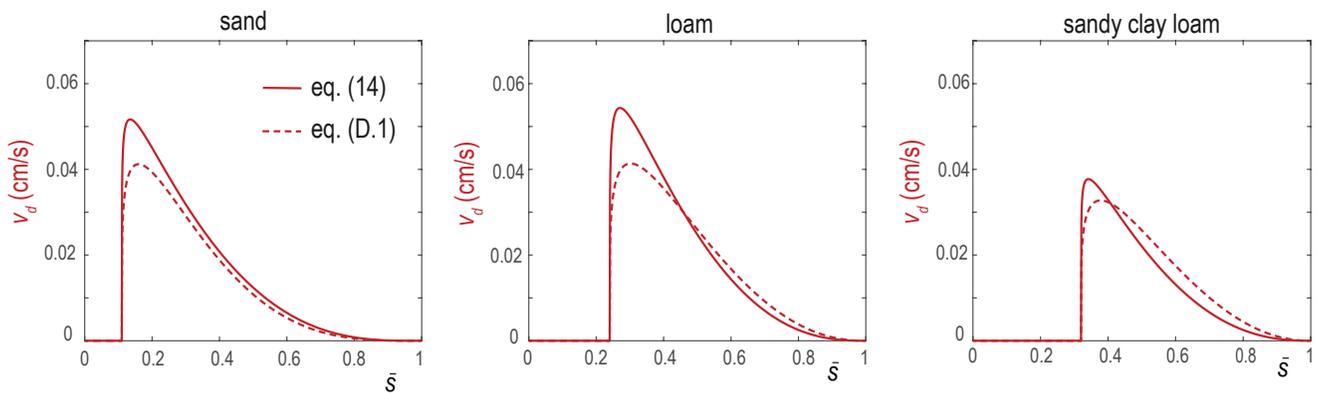
Figure B1. Comparison of the deposition velocity v_d from Equation B1 (Ehhalt & Rohrer, 2013) and Equation 14 ($\ell = 1$ cm, $Z = 10$ cm, and $T = 30°$C).

Appendix C: Equilibrium Relationships With P

Retaining the production term P in Equation 4 under the quasi-steady approximation, one obtains:

$$\bar{c}(t) = \frac{c_a + Z\,P/g_T}{1 + v_{BD}/g_T},\tag{C1}$$

and

$$v_d = \frac{v_{BD} - Z\,P/c_a}{1 + v_{BD}/g_T}.\tag{C2}$$

The latter shows that the soil becomes a source of hydrogen if $Z\,P > c_a v_{BD}$.

Data Availability Statement

Data sets for this research are available in Conrad and Seiler (1981), Meredith (2016), Meredith et al. (2017), PBO (2020), Rodell et al. (2004), and Smith-Downey et al. (2006).

References

Bay, S. K., Dong, X., Bradley, J. A., Leung, P. M., Grinter, R., & Jirapanjawat, T., et al. (2021). Trace gas oxidizers are widespread and active members of soil microbial communities. *Nature Microbiology*, 1–11. https://doi.org/10.1038/s41564-020-00811-w

Benjamin, J. R., & Cornell, C. A. (2014). *Probability, statistics, and decision for civil engineers*. Courier Corporation.

Brady, N. C., Weil, R. R., & Weil, R. R. (2008). *The nature and properties of soils* (Vol. 13). Prentice Hall.

Campbell, G. S. (1974). A simple method for determining unsaturated conductivity from moisture retention data. *Soil Science*, *117*(6), 311–314. https://doi.org/10.1097/00010694-197406000-00001

Chaney, N. W., Van Huijgevoort, M. H., Shevliakova, E., Malyshev, S., Milly, P. C., Gauthier, P. P., & Sulman, B. N. (2018). Harnessing big data to rethink land heterogeneity in earth system models. *Hydrology and Earth System Sciences*, *22*(6), 3311–3330. https://doi.org/10.5194/hess-22-3311-2018

Clapp, R. B., & Hornberger, G. M. (1978). Empirical equations for some soil hydraulic properties. *Water Resources Research*, *14*(4), 601–604. https://doi.org/10.1029/wr014i004p00601

Conrad, R., & Seiler, W. (1980). Contribution of hydrogen production by biological nitrogen fixation to the global hydrogen budget. *Journal of Geophysical Research*, *85*(C10), 5493–5498. https://doi.org/10.1029/jc085ic10p05493

Conrad, R., & Seiler, W. (1981). Decomposition of atmospheric hydrogen by soil microorganisms and soil enzymes. *Soil Biology and Biochemistry*, *13*(1), 43–49. https://doi.org/10.1016/0038-0717(81)90101-2

Conrad, R., & Seiler, W. (1985). Influence of temperature, moisture, and organic carbon on the flux of H_2 and CO between soil and atmosphere: Field studies in subtropical regions. *Journal of Geophysical Research*, *90*(D3), 5699–5709. https://doi.org/10.1029/jd090id03p05699

Constant, P., Chowdhury, S. P., Pratscher, J., & Conrad, R. (2010). Streptomycetes contributing to atmospheric molecular hydrogen soil uptake are widespread and encode a putative high-affinity [NiFe]-hydrogenase. *Environmental Microbiology*, *12*(3), 821–829. https://doi.org/10.1111/j.1462-2920.2009.02130.x

Constant, P., Poissant, L., & Villemur, R. (2009). Tropospheric H_2 budget and the response of its soil uptake under the changing environment. *The Science of the Total Environment*, *407*(6), 1809–1823. https://doi.org/10.1016/j.scitotenv.2008.10.064

Derwent, R. G., Stevenson, D. S., Utembe, S. R., Jenkin, M. E., Khan, A. H., & Shallcross, D. E. (2020). Global modelling studies of hydrogen and its isotopomers using STOCHEM-CRI: Likely radiative forcing consequences of a future hydrogen economy. *International Journal of Hydrogen Energy*, *45*(15), 9211–9221. https://doi.org/10.1016/j.ijhydene.2020.01.125

Dingman, S. L. (2015). *Physical hydrology*. Waveland press.

Ehhalt, D., & Rohrer, F. (2009). The tropospheric cycle of H_2: A critical review. *Tellus B: Chemical and Physical Meteorology*, *61*(3), 500–535. https://doi.org/10.1111/j.1600-0889.2009.00416.x

Ehhalt, D., & Rohrer, F. (2011). The dependence of soil H_2 uptake on temperature and moisture: A reanalysis of laboratory data. *Tellus B: Chemical and Physical Meteorology*, *63*(5), 1040–1051. https://doi.org/10.1111/j.1600-0889.2011.00581.x

Ehhalt, D., & Rohrer, F. (2013). Deposition velocity of H_2: A new algorithm for its dependence on soil moisture and temperature. *Tellus B: Chemical and Physical Meteorology*, *65*(1), 19904. https://doi.org/10.3402/tellusb.v65i0.19904

FAO. (2009). *Global map of aridity – 10 arc minutes*. Retrieved from http://www.fao.org/geonetwork/srv/en/metadata.show?id=37040

Feng, X., Porporato, A., & Rodriguez-Iturbe, I. (2013). Changes in rainfall seasonality in the tropics. *Nature Climate Change*, *3*(9), 811–815. https://doi.org/10.1038/nclimate1907

Fischer, E. M., Sedláček, J., Hawkins, E., & Knutti, R. (2014). Models agree on forced response pattern of precipitation and temperature extremes. *Geophysical Research Letters*, *41*(23), 8554–8562. https://doi.org/10.1002/2014gl062018

Greening, C., Constant, P., Hards, K., Morales, S. E., Oakeshott, J. G., Russell, R. J., et al. (2015). Atmospheric hydrogen scavenging: From enzymes to ecosystems. *Applied and Environmental Microbiology*, *81*(4), 1190–1199. https://doi.org/10.1128/aem.03364-14

Hydrogen Council. (2020). *Path to hydrogen competitiveness: A cost perspective*. https://www.h2knowledgecentre.com/content/policypaper1202?crawler=redirect&mimetype=application/pdf

Internation Energy Agency (IEA). (2019). *The future of hydrogen* (Technical Report). https://www.iea.org/reports/the-future-of-hydrogen

Ji, M., Greening, C., Vanwonterghem, I., Carere, C. R., Bay, S. K., Steen, J. A., et al. (2017). Atmospheric trace gases support primary production in Antarctic desert surface soil. *Nature*, *552*(7685), 400–403. https://doi.org/10.1038/nature25014

Jordaan, K., Lappan, R., Dong, X., Aitkenhead, I. J., Bay, S. K., Chiri, E., et al. (2020). Hydrogen-oxidizing bacteria are abundant in desert soils and strongly stimulated by hydration. *mSystems*, *5*(6). https://doi.org/10.1128/msystems.01131-20

Khalil, M., & Rasmussen, R. (1990). Global increase of atmospheric molecular hydrogen. *Nature*, *347*(6295), 743–745. https://doi.org/10.1038/347743a0

Khdhiri, M., Hesse, L., Popa, M. E., Quiza, L., Lalonde, I., Meredith, L. K., et al. (2015). Soil carbon content and relative abundance of high affinity H_2-oxidizing bacteria predict atmospheric H_2 soil uptake activity better than soil microbial community composition. *Soil Biology and Biochemistry*, *85*, 1–9. https://doi.org/10.1016/j.soilbio.2015.02.030

Khdhiri, M., Piché-Choquette, S., Tremblay, J., Tringe, S. G., & Constant, P. (2017). The tale of a neglected energy source: Elevated hydrogen exposure affects both microbial diversity and function in soil. *Applied and Environmental Microbiology*, *83*(11). https://doi.org/10.1128/aem.00275-17

King, G. M. (2017). *Water potential as a master variable for atmosphere-soil trace gas exchange in arid and semiarid ecosystems* (pp. 31–46). The biology of arid soils. https://doi.org/10.1515/9783110419047-003

La Favre, J., & Focht, D. (1983). Conservation in soil of H_2 liberated from N_2 fixation by Hup-nodules. *Applied and Environmental Microbiology*, *46*(2), 304–311. https://doi.org/10.1128/aem.46.2.304-311.1983

Laio, F., Porporato, A., Ridolfi, L., & Rodriguez-Iturbe, I. (2001). Plants in water-controlled ecosystems: Active role in hydrologic processes and response to water stress: II. Probabilistic soil moisture dynamics. *Advances in Water Resources*, *24*(7), 707–723. https://doi.org/10.1016/s0309-1708(01)00005-7

Lallo, M., Aalto, T., Laurila, T., & Hatakka, J. (2008). Seasonal variations in hydrogen deposition to boreal forest soil in southern Finland. *Geophysical Research Letters*, *35*(4). https://doi.org/10.1029/2007gl032357

Larson, K. M., Small, E. E., Gutmann, E. D., Bilich, A. L., Braun, J. J., & Zavorotny, V. U. (2008). Use of GPS receivers as a soil moisture network for water cycle studies. *Geophysical Research Letters*, *35*(24). https://doi.org/10.1029/2008gl036013

Leung, P. M., Bay, S. K., Meier, D. V., Chiri, E., Cowan, D. A., & Gillor, O., et al. (2020). Energetic basis of microbial growth and persistence in desert ecosystems. *mSystems*, *5*(2). https://doi.org/10.1128/msystems.00495-19

Lubitz, W., Ogata, H., Rüdiger, O., & Reijerse, E. (2014). Hydrogenases. *Chemical Reviews*, *114*(8), 4081–4148. https://doi.org/10.1021/cr4005814

Manzoni, S., Schimel, J. P., & Porporato, A. (2012). Responses of soil microbial communities to water stress: Results from a meta-analysis. *Ecology*, *93*(4), 930–938. https://doi.org/10.1890/11-0026.1

Meredith, L. K. (2016). *Fluxes of molecular hydrogen (H_2) at the Harvard Forest EMS Tower in 2011*. Retrieved from http://harvardforest.fas.harvard.edu:8080/exist/apps/datasets/showData.html?id=hf288

Meredith, L. K., Commane, R., Keenan, T. F., Klosterman, S. T., Munger, J. W., Templer, P. H., et al. (2017). Ecosystem fluxes of hydrogen in a mid-latitude forest driven by soil microorganisms and plants. *Global Change Biology*, *23*(2), 906–919. https://doi.org/10.1111/gcb.13463

Meredith, L. K., Rao, D., Bosak, T., Klepac-Ceraj, V., Tada, K. R., Hansel, C. M., et al. (2014). Consumption of atmospheric hydrogen during the life cycle of soil-dwelling actinobacteria. *Environmental Microbiology Reports*, *6*(3), 226–238. https://doi.org/10.1111/1758-2229.12116

Millington, R., & Quirk, J. (1961). Permeability of porous media. *Nature*, *183*(4658), 387–388. https://doi.org/10.1038/183387a0

Moldrup, P., Chamindu Deepagoda, T., Hamamoto, S., Komatsu, T., Kawamoto, K., Rolston, D. E., & de Jonge, L. W. (2013). Structure-dependent water-induced linear reduction model for predicting gas diffusivity and tortuosity in repacked and intact soil. *Vadose Zone Journal*, *12*(3), 1–11. https://doi.org/10.2136/vzj2013.01.0026

Moldrup, P., Olesen, T., Yamaguchi, T., Schjønning, P., & Rolston, D. (1999). Modeling diffusion and reaction in soils: IX. The Buckingham-Burdine-Campbell equation for gas diffusivity in undisturbed soil. *Soil Science*, *164*(8), 542–551. https://doi.org/10.1097/00010694-199908000-00002

Moldrup, P., Olesen, T., Yoshikawa, S., Komatsu, T., & Rolston, D. E. (2004). Three-porosity model for predicting the gas diffusion coefficient in undisturbed soil. *Soil Science Society of America Journal*, *68*(3), 750–759. https://doi.org/10.2136/sssaj2004.7500

Morfopoulos, C., Foster, P., Friedlingstein, P., Bousquet, P., & Prentice, I. (2012). A global model for the uptake of atmospheric hydrogen by soils. *Global Biogeochemical Cycles*, *26*(3). https://doi.org/10.1029/2011gb004248

Novelli, P. C., Lang, P. M., Masarie, K. A., Hurst, D. F., Myers, R., & Elkins, J. W. (1999). Molecular hydrogen in the troposphere: Global distribution and budget. *Journal of Geophysical Research*, *104*(D23), 30427–30444. https://doi.org/10.1029/1999jd900788

Paulot, F., Malyshev, S., Nguyen, T., Crounse, J. D., Shevliakova, E., & Horowitz, L. W. (2018). Representing sub-grid scale variations in nitrogen deposition associated with land use in a global earth system model: Implications for present and future nitrogen deposition fluxes over North America. *Atmospheric Chemistry and Physics*, *18*(24), 17963–17978. https://doi.org/10.5194/acp-18-17963-2018

Paulot, F., Paynter, D., Naik, V., Malyshev, S., Menzel, R., & Horowitz, L. (2021). Global modeling of hydrogen using GFDL-AM4.1: Sensitivity of soil removal and radiative forcing. *International Journal of Hydrogen Energy*, *46*(24), 13446–13460. https://doi.org/10.1016/j.ijhydene.2021.01.088

PBO. (2020). *PBO H_2O data portal, station sdhl*. Retrieved from https://cires1.colorado.edu/portal/?station=sdhl

Piché-Choquette, S., & Constant, P. (2019). Molecular hydrogen, a neglected key driver of soil biogeochemical processes. *Applied and Environmental Microbiology*, *85*(6). https://doi.org/10.1128/aem.02418-18

Pieterse, G., Krol, M., Batenburg, A., Brenninkmeijer, M., Popa, M., O'doherty, S., et al. (2013). Reassessing the variability in atmospheric H_2 using the two-way nested TM5 model. *Journal of Geophysical Research: Atmospheres*, *118*(9), 3764–3780. https://doi.org/10.1002/jgrd.50204

Porporato, A., Laio, F., Ridolfi, L., & Rodriguez-Iturbe, I. (2001). Plants in water-controlled ecosystems: Active role in hydrologic processes and response to water stress: III. Vegetation water stress. *Advances in Water Resources*, *24*(7), 725–744. https://doi.org/10.1016/s0309-1708(01)00006-9

Rhee, T., Brenninkmeijer, C., & Röckmann, T. (2006). The overwhelming role of soils in the global atmospheric hydrogen cycle. *Atmospheric Chemistry and Physics*, *6*(6), 1611–1625. https://doi.org/10.5194/acp-6-1611-2006

Robson, R. L., & Postgate, J. R. (1980). Oxygen and hydrogen in biological nitrogen fixation. *Annual Reviews in Microbiology*, *34*(1), 183–207. https://doi.org/10.1146/annurev.mi.34.100180.001151

Rodell, M., Houser, P., Jambor, U., Gottschalck, J., Mitchell, K., Meng, C.-J., et al. (2004). The global land data assimilation system. *Bulletin of the American Meteorological Society*, *85*(3), 381–394. https://doi.org/10.1175/bams-85-3-381

Rodriguez-Iturbe, I., Porporato, A., Ridolfi, L., Isham, V., & Coxi, D. (1999). Probabilistic modelling of water balance at a point: The role of climate, soil and vegetation. *Proceedings of the Royal Society of London. Series A: Mathematical, Physical and Engineering Sciences*, *455*, 3789–3805. https://doi.org/10.1098/rspa.1999.0477

Sander, R. (2015). Compilation of Henry's law constants (version 4.0) for water as solvent. *Atmospheric Chemistry and Physics*, *15*(8), 4399–4981. https://doi.org/10.5194/acp-15-4399-2015

Schmitt, S., Hanselmann, A., Wollschläger, U., Hammer, S., & Levin, I. (2009). Investigation of parameters controlling the soil sink of atmospheric molecular hydrogen. *Tellus B: Chemical and Physical Meteorology*, *61*(2), 416–423. https://doi.org/10.1111/j.1600-0889.2008.00402.x

Simmonds, P., Derwent, R., Manning, A., Grant, A., O'doherty, S., & Spain, T. (2011). Estimation of hydrogen deposition velocities from 1995–2008 at mace head, Ireland using a simple box model and concurrent ozone depositions. *Tellus B: Chemical and Physical Meteorology*, *63*(1), 40–51. https://doi.org/10.1111/j.1600-0889.2010.00518.x

Smith-Downey, N. V., Randerson, J. T., & Eiler, J. M. (2006). Temperature and moisture dependence of soil H_2 uptake measured in the laboratory. *Geophysical Research Letters*, *33*(14). https://doi.org/10.1029/2006gl026749

Smith-Downey, N. V., Randerson, J. T., & Eiler, J. M. (2008). Molecular hydrogen uptake by soils in forest, desert, and marsh ecosystems in California. *Journal of Geophysical Research*, *113*(G3). https://doi.org/10.1029/2008jg000701

Tromp, T. K., Shia, R.-L., Allen, M., Eiler, J. M., & Yung, Y. L. (2003). Potential environmental impact of a hydrogen economy on the stratosphere. *Science*, *300*(5626), 1740–1742. https://doi.org/10.1126/science.1085169

Warwick, N., Bekki, S., Nisbet, E., & Pyle, J. (2004). Impact of a hydrogen economy on the stratosphere and troposphere studied in a 2-D model. *Geophysical Research Letters*, *31*(5). https://doi.org/10.1029/2003gl019224

Yashiro, H., Sudo, K., Yonemura, S., & Takigawa, M. (2011). The impact of soil uptake on the global distribution of molecular hydrogen: Chemical transport model simulation. *Atmospheric Chemistry and Physics Discussions*, *11*(2). https://doi.org/10.5194/acp-11-6701-2011

Yin, J., Porporato, A., D'Odorico, P., & Rodríguez-Iturbe, I. (2019). Ecohydrology. *Encyclopedia of Water: Science, Technology, and Society*, 1–21. https://doi.org/10.1002/9781119300762.wsts0026

Yonemura, S., Kawashima, S., & Tsuruta, H. (2000). Carbon monoxide, hydrogen, and methane uptake by soils in a temperate arable field and a forest. *Journal of Geophysical Research*, *105*(D11), 14347–14362. https://doi.org/10.1029/1999jd901156

Yonemura, S., Yokozawa, M., Kawashima, S., & Tsuruta, H. (2000). Model analysis of the influence of gas diffusivity in soil on CO and H_2 uptake. *Tellus B: Chemical and Physical Meteorology*, *52*(3), 919–933. https://doi.org/10.3402/tellusb.v52i3.17075